Program Digest, 2019 IEEE International Ultrasonics Symposium (IUS)
Glasgow, Scotland, October 6-9, 2019

Ultrasonic Characterization of Spatially Varying Material Properties in Metal Components Fabricated by Additive Manufacturing

Kenneth Walton
Department of Chemical Engineering
University of Utah
Salt Lake City, United States
kenneth.walton@utah.edu

Mikhail Skliar
Department of Chemical Engineering
University of Utah
Salt Lake City, United States
mikhail.skliar@utah.edu

***Abstract*— We investigated the sensitivity of ultrasonic measurements to changes in the operating conditions during additive fabrication for 316L stainless steel samples by selective laser melting. We found that the velocity of the ultrasound propagation positively correlates with the energy density used to melt layers of metal powder during the fabrication. In the range of the investigated conditions, the faster ultrasonic propagation, observed with the increase in the energy density, was shown to correspond to the improved hardness and the modulus of 316L stainless steel. Overall, our results indicate the feasibility of ultrasonic characterization of heterogeneities in material properties of metal components produced by additive manufacturing.**

***Keywords*— Ultrasonic Evaluation, Material Properties, Additive Manufacturing, Selective Laser Melting, NDE**

I. INTRODUCTION

Selective laser melting (SLM) is an additive manufacturing technique which fabricates components layer-by-layer by melting layers of powder by a high-power laser beam. This method can produce parts with complex internal and surface geometries beyond what is possible with traditional fabrication methods. During the fabrication process by SLM, as new powder layers are deposited and then melted by a laser, previously formed layers close to the current plane scanned by a laser are re-heated. These repeated heating cycles differ with the position, which may cause spatial variability in material properties in the direction of the build and between the interior and the edges of the part [1-4]. Heterogeneity in densities, undesirable in most applications, may be characterized noninvasively by X-ray computed tomography. X-ray CT can also image microstructure heterogeneity, but only in small samples.

Ultrasound is an appealing modality in the characterization of mechanical properties of additively manufactured (AM) parts. Changes in several material properties impact the speed of ultrasound in solids, v:

$$v = \sqrt{\frac{E(1-\mu)}{\rho(1+\mu)(1-2\mu)}} \quad (1)$$

where E is the Young modulus, μ is the Poisson's ratio, and ρ is density. Any deviation in the speed of sound (SOS) along the path of ultrasonic propagation will reflect the changes in E, ρ, or μ or the combination of the three. If we use the pulse-echo mode, then v can be found as

$$v = \frac{2L}{t_{of}} \quad (2)$$

where t_{of} is the measured time of flight (TOF) of the ultrasound pulse and L is the length of the ultrasound propagation from a transducer to a feature creating a return echo. The obtained SOS will indicate changes in the material properties along the path of propagation but will not reveal if spatial heterogeneity of properties is present.

Temperature is yet another property that changes SOS. We have previously developed a method for ultrasonic measurements of temperature distribution in solid [5-7] and adapted its concept to the material characterization of SLM-manufactured components [8]. While the adaption was shown to be feasible, no heterogeneity was detected in a 3D-printed 31AL aluminum alloy sample used in experiments. In concert with ultrasound results, the measured elastic modulus, surface morphology imaged by SEM, and the X-ray CT did not reveal heterogeneities the aluminum sample used in experiments.

The goal of the current study is to investigate the sensitivity of SOS measurements to changes in the operating conditions during SLM fabrication for stainless steel samples, which are compositionally more complex that an aluminum alloy used in [8], and for which thermal-cycling-induced heterogeneity was reported previously [1,3,4]. To that end, we used a varying energy density in the build direction to fabricate stainless-steel samples. The ultrasound characterization of the samples revealed that the SOS is positively correlated with the energy density, which was found to affect the hardness and the reduced modulus. The ultrasound measurements also indicated the anisotropy of material properties in the build and the orthogonal directions.

II. METHOD

A. 3D Printed Sample

Three samples with the rectangular cross-section (30-by-30 mm) and ~50 mm height in the build direction were fabricated from 316L stainless steel powder by selective laser melting

The authors acknowledge financial support from the NETL of the U.S. Department of Energy under award number DE-FE0031559.

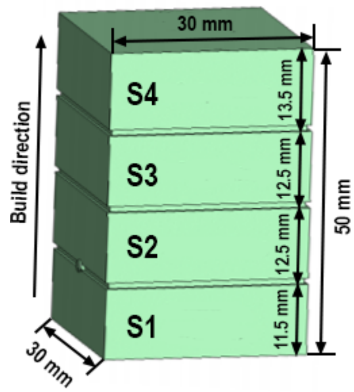

Fig. 1: Geometry and segmentation of SLM-fabricated stainless-steel samples.

(EOS M 280). Each sample consisted of four segments shown in Fig. 1, dimensions of which varied slightly between the samples. One of the parts was fabricated with a constant energy density of 33 J/mm^3 in all segments applied to a layer of powder 40 μm thick. At these conditions, in addition to the powder, ~50 μm of already "printed" material below the build plane is re-melted. The S1 segments of the other two samples were fabricated with the same power density. Sections S2, S3, and S4 of the second sample (referred to as V+ sample) were printed with the beam power and scanning rate adjusted to increase the energy densities by 3 J/mm^3 for each new section (Table 1). The V- sample was fabricated by reducing the power density by the same 3 J/mm^3 in different segments in the build direction.

B. Ultrasonic Measurements

The ultrasound excitation was created by a transducer (Olympus IMS, model V110; 0.2" diameter, 5 MHz central frequency) connected to a pulser/receiver (model 5077PR, Olympus IMS). The pulse-echo measurements averaged in the build direction were obtained by coupling the transducer to the top or bottom faces of the samples. The measurements for different segments were obtained by coupling the transducer to the sides of the samples, centering it in the middle of each section. Grooves on the sides of the samples (0.5-mm deep) provided the reference when positioning the transducer.

The echoes' waveforms were acquired with a high-speed digitizer (PicoScope 6407). The waveforms used in the signal analysis were obtained by averaging 32 raw waveforms captured under identical conditions.

C. TOF Measurements

The TOF in different directions was found by cross-correlation of the envelope of echoes' waveforms after the first and the second pass of the ultrasonic excitation through the sample [6-8]. The calculation the SOS by equation (2) requires the length of the ultrasound propagation. The overall height of samples in the build direction, L, and the dimensions of segments were measured by a micrometer. The SOS within different segments was obtained using TOF measurements normal to the build direction.

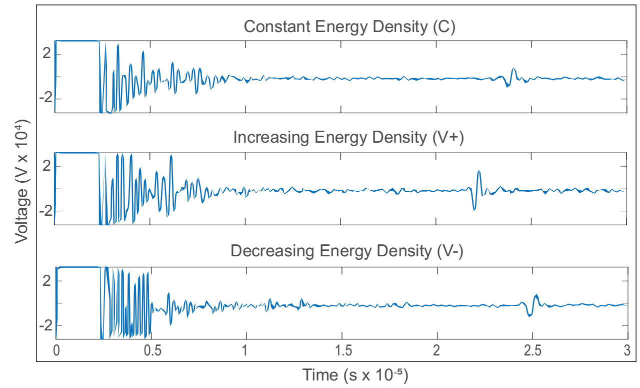

Fig. 2: Ultrasonic propagation in the build direction. The waveforms show faster arrival of the ultrasonic signal in the V+ sample and the increase in the TOF in the V- sample.

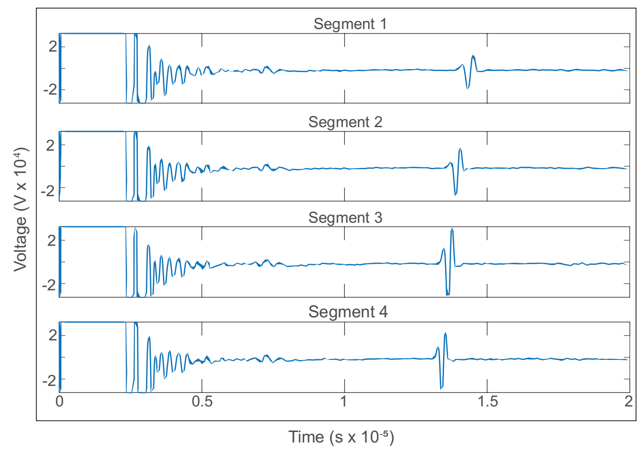

Fig. 3: Ultrasound propagation across the segments of the sample V+ (orthogonal to the build direction). Note the reduction in the echoes' time of flight with the segment's number.

Table 1: Laser power, scan speed, and energy density.

Sample		**Hatching Settings**		
		Power, W	Speed of laser rastering, $\frac{mm}{s}$	Energy density, $\frac{J}{mm^3}$
Constant energy	S1-4	350	2650	33
V+: Increasing energy density	S1	350	2650	33
	S2	355	2465	36
	S3	360	2310	39
	S4	365	2175	42
V-: Decreasing energy density	S1	350	2650	33
	S2	300	2500	30
	S3	250	2315	27
	S4	200	2085	24

D. Measurements of Mechanical Properties

The samples were mechanically polished on each side, and the nano-indenter (Hysitron TI Premier, Bruker) was used to measure the hardness and reduced modulus of the material in all segments.

III. RESULTS

Figure 2 shows the echoes' waveforms after the ultrasound excitation passes through the three analyzed samples in the direction of the build. In this case, the elastic waves propagate through all four segments, and the material properties of each segment impact the echoes' arrival time. The inspection of the arrival time indicates that the TOF is longer, and the average SOS is smaller in the V- sample with segments processed at lower power density. The elevated power density in V+ sample leads to a shorter TOF and faster average ultrasound propagation. Table 2 gives a quantitative summary of these observations.

Table 2: TOF and average SOS in the build direction.

	Samples		
	Constant energy density	V+	V-
Hight (mm)	49.6189	49.7205	49.4538
TOF (μs)	21.082	19.317	21.875
SOS (m/s)	4707.318	5147.902	4511.220

The impact of energy density, determined by the SLM fabrication parameters listed in Table 2, on the SOS was determined by measuring the TOF for different segments when the ultrasound excitation was applied in the direction normal to the one in which the parts were built. Figure 3 shows the pulse-echo response of the material printed with different energy densities, which we obtained after coupling the transducer to the sides of part V+ (energy density increases with the segment number) in the middle of each segment. The inspection of the arrival times for echoes propagating across different segments, each with the same cross-section, indicates that as the energy density increased in the build direction, from Segment 1 to Segment 4, the time of flight shortens, and the speed of the ultrasound propagation becomes faster. The results for V- sample (energy density decreases in the build direction), shown in Figure 4, support this conclusion.

Table 3: Speed of sound in segments of different samples.

Sample	***Property***	***S1***	***S2***	***S3***	***S4***
Constant energy density	Length, mm	29.7180	29.7561	29.7815	29.7561
	TOF, μs	11.9744	11.9328	11.92	11.8912
	SOS, m/s	**4963.58**	**4987.27**	**4996.85**	**5004.72**
V+	Length, mm	29.7688	29.7942	29.7688	29.7688
	TOF, μs	11.8496	11.3072	11.0816	19.3168
	SOS, m/s	**5024.44**	**5269.95**	**5372.65**	**5519.28**
V-	Length, mm	29.8069	29.8196	29.8196	29.8196
	TOF, μs	11.8496	11.3072	11.0816	10.7872
	SOS, m/s	**5024.44**	**5269.95**	**5372.65**	**5519.28**

The positive correlation between the SOS and the applied energy density seen in Figures 3 and 4 is gauged by the data in Table 3 which lists the SOS computed from equation (2) using the TOF and dimensional measurements for different segments of V+, V-, and constant energy density samples.

The correlation between energy density and the mechanical properties of stainless steel in different segments was established using nano-indenter measurements. Table 4 summarizes the results that indicate that at the investigated fabrication conditions, the hardness and the modulus of stainless steel increase with the energy density.

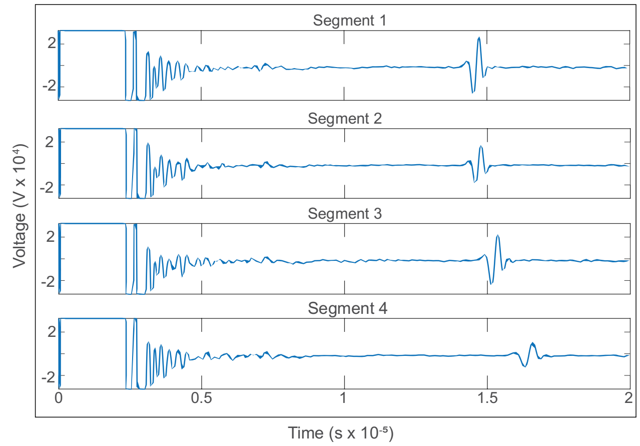

Fig. 4: Ultrasound propagation normal to the build directions across the segments of sample V-. The echoes' time of flight increases with the segment's number.

Table 4: Mechanical properties in segments of different samples.

Sample	Hardness and Reduced Modulus in GPa±std				
	Property	***S1***	***S2***	***S3***	***S4***
Constant energy density	Hardness	5.770 ±0.836	5.783 ±0.632	6.107 ±0.585	5.748 ±1.231
	Reduced Modulus	185.043 ±11.433	186.388 ±18.031	188.764 ±19.118	181.584 ±15.461
V+	Hardness	5.738 ±1.302	6.043 ±0.746	6.298 ±1.465	6.877 ±1.737
	Reduced Modulus	181.722 ±12.446	183.780 ±10.815	190.836 ±23.100	198.858 ±16.714
V-	Hardness	7.427 ±1.501	6.222 ±0.446	5.844 ±0.809	4.335 ±1.238
	Reduced Modulus	187.817 ±17.103	186.406 ±17.396	173.883 ±15.706	150.206 ±18.447

IV. DISCUSSION

The energy density during selective laser melting is the critically important processing parameter that may be controlled by modulating the power of the scanning laser, the speed of pattern rastering, and the thickness of the powder layer. In the range of the investigated conditions used in the additive fabrication of metal components from metallic powder by a computer-controlled SLM, the energy density positively correlated with the hardness and the modulus of 316L stainless steel, the grade often used when improved corrosion resistance and strength at elevated temperatures are required. The velocity of the ultrasound propagation was found to be sensitive to these changes in material properties, and the positive correlation with the energy density.

Overall, our results indicate the feasibility of ultrasonic characterization of heterogeneities in the material properties of 3D-printed metal parts.

REFERENCES

[1] Y. Liu, Z. Pang, and J. Zhang, "Comparative study on the influence of subsequent thermal cycling on microstructure and mechanical properties of selective laser melted 316L stainless steel," Appl. Phys. A, vol. 123, no. 11, p. 688, November 2017.

[2] K. Kunze, T. Etter, J. Grässlin, and V. Shklover, "Texture , anisotropy in microstructure and mechanical properties of IN738LC alloy processed by selective laser melting (SLM)," *Mater. Sci. Eng. A*, vol. 620, pp. 213–222, 2014.

[3] S. Das, D. L. Bourell, and S. S. Babu, "Metallic materials for 3D printing," *MRS Bulletin*, Vol 41, issue 10, pp. 729–741, October 2016.

[4] M. Yakout, M. A. Elbestawi, and S. C. Veldhuis, "Density and mechanical properties in selective laser melting of Invar 36 and stainless steel 316L," *J. Mater. Process. Tech.*, vol. 266, no. July 2018, pp. 397–420, 2018.

[5] Y. Jia, V. Chernyshev, and M. Skliar, "Ultrasound measurements of segmental temperature distribution in solids: Method and its high temperature validation," Ultrasonics, vol. 66, pp. 91–102, March 2016.

[6] Y. Jia and M. Skliar, "Noninvasive ultrasound measurements of temperature distribution and heat fluxes in solids," Energy and Fuels, vol. 30, pp. 4363–4371, no. 5, May 2016.

[7] M. Skliar, K. Whitty, and A. Butterfield, "Ultrasonic temperature measurement device," US Patents 8,801,277 B2, 2014, and 9,212,956, 2015.

[8] M. Roy, K. Walton, J. B. Harley and M. Skliar, "Ultrasonic Evaluation of Segmental Variability in Additively Manufactured Metal Components," *2018 IEEE International Ultrasonics Symposium (IUS)*, Kobe, 2018, pp. 1-4, October 2018.